ingegneria sismica
International Journal of Earthquake Engineering
Anno XLIII - Num. 1 - 2026

Research on Data Analysis and Optimization Algorithms for Building Structural Performance Monitoring in the Context of Intelligent Construction

Tairan Zhang[1,*]

[1] School of Civil and Environmental Engineering, Nanyang Technological University 50 Nanyang Avenue, Singapore 639798, Singapore

SUMMARY: *Under the continuous advancement of new urbanization, the complexity of building structures has been increasing, and the traditional safety management model relying on manual inspection and single-point monitoring has been unable to meet the monitoring requirements for structural performance under intelligent construction conditions. This paper addresses the heterogeneity of multi-source monitoring data and noise interference, and constructs an analysis framework integrating preprocessing, bidirectional temporal modeling of structural perception, and multi-objective optimization. It introduces a multi-scale attention mechanism and an improved particle swarm algorithm to jointly optimize key parameters. Based on three types of engineering monitoring data sets, experiments show that this method reduces the health degree prediction error to 0.074, with an accuracy rate of 93.8% and an F1 value of 92.7%, which is approximately 2% higher than the optimal comparison model. It also maintains good robustness and real-time performance even under noise enhancement and missing monitoring points, and has application value for building structure safety monitoring in the context of intelligent construction.*
Povzetek: For the structural safety monitoring under the conditions of intelligent construction, this paper constructs an integrated analysis and optimization framework for multi-source monitoring data, integrating hierarchical coding, time series modeling and multi-objective optimization, to achieve the joint assessment of structural health and status level. The engineering measurement results show that this method reduces the health degree prediction error to 0.074 and increases the accuracy rate to 93.8%. It still has good robustness and real-time performance even in the scenarios of enhanced noise and missing monitoring points, providing technical support for the full life cycle monitoring and intelligent operation and maintenance decision-making of building structures.

KEYWORDS: *Intelligent construction; Monitoring of building structural performance; Multi-source structural monitoring data; Time series modeling; State assessment; Optimization algorithm*

1 Introduction

In recent years, with the continuous advancement of new urbanization and infrastructure construction, the volume of building structures has been increasing and their functional complexity has been continuously rising. The traditional safety management model that relies on manual inspection and decentralized monitoring has been unable to meet the requirements

*13396196797@163.com
https://doi.org/10.65102/is2026075 Published: 30 April, 2026

of real-time perception and refined control of structural performance. The intelligent construction mode supported by Internet of Things, BIM, cloud computing, and digital twin provides a technical foundation for the automatic collection, centralized management, and coordinated decision-making of structural performance monitoring data. A large amount of time-series data from multiple sensors such as acceleration, displacement, strain, and temperature can be continuously accumulated during the construction and operation phases. How to extract the evolution patterns of structural performance from these complex monitoring data, timely identify potential risks, and provide reliable input for intelligent decision-making systems has become an important issue in the field of intelligent construction.

Existing research has established a certain foundation in the field of building structure health monitoring and performance assessment, including threshold discrimination methods based on empirical indicators, state recognition methods using statistical features or traditional machine learning models, and some time-series prediction models for the degradation process of structures. However, in the intelligent construction scenario, multi-source monitoring data has the characteristics of strong coupling, high dimensionality, and variable working conditions. Simple analysis methods relying on a single sensor or local indicators are difficult to comprehensively reflect the overall performance of the structure; at the same time, model parameter settings often rely on empirical adjustments, and the adaptability to different engineering objects and working conditions is insufficient, lacking a systematic optimization mechanism for multiple objectives such as monitoring accuracy, robustness, and computational cost.

Based on the above background, this paper focuses on the monitoring data analysis and optimization algorithm design as the two core issues in the performance monitoring of building structures in the intelligent construction environment. On one hand, it constructs a multi-source monitoring data preprocessing and feature representation method considering structural topological relationships and construction conditions information, improving the ability of data to represent the state of structural performance; on the other hand, it designs an algorithm framework integrating time-series modeling and state assessment, and introduces optimization strategies to jointly optimize model hyperparameters and monitoring configurations, taking into account prediction accuracy, robustness, and real-time engineering application. Through engineering data verification, it is expected to provide a scalable technical path and method support for the construction of a building structure performance monitoring system in the intelligent construction context.

2 Related Work

In recent years, research on intelligent monitoring and performance assessment of engineering structures has been continuously emerging. Fan et al. [1] systematically reviewed the application progress of data-driven and intelligent algorithms in the study of concrete structure cracks, indicating that methods such as deep learning and pattern recognition have significantly improved the automation and detection accuracy in crack identification, segmentation, and damage assessment, providing important support for the intelligent identification of apparent damage of structures. However, such research mostly focuses on a single damage form or local component image features, and pays less attention to the time-series monitoring data from multiple sensors and its relationship with the evolution of overall structural performance.

In the context of intelligent construction and Building Information Modeling (BIM), a large number of works have introduced data-driven methods and optimization algorithms into the design and construction process optimization of structures. Li and Zhang [2] combined BIM with reinforcement learning to optimize the scheduling of complex building structure construction processes, continuously improving the construction sequence and resource allocation based on environmental feedback, demonstrating the potential of intelligent decision-making in the construction process under big data conditions. Huang et al. [3] based on BIM and data-driven multi-objective optimization methods, systematically optimized the structure combination of asphalt pavement, achieving a trade-off between performance and cost. Zhang et al. [4] developed a parametric structural design tool for super high-rise buildings based on Grasshopper and intelligent algorithms, enabling the linkage adjustment of structural parameters and performance indicators, and enhancing the design efficiency and exploratory space at the scheme stage of high-rise buildings. Li [5] conducted research on building structure design optimization using genetic algorithms, improving the safety and economy of structural design schemes through encoding and evolutionary search of variables such as section dimensions and component layouts. Pham et al. [6] addressed the issue of residential space ground paving, proposing a floor tile layout design method combining nested algorithms and multi-objective optimization, and conducting comprehensive optimization of layout and material utilization based on BIM data. Golmaei et al. [7] introduced the whale algorithm into construction progress optimization combined with BIM, obtaining a better construction progress plan through intelligent search and improving the balance between project duration and resource utilization. Jin [8] started from the construction equipment level, using reinforcement learning algorithms to achieve path planning and motion control for building robots, providing new ideas for autonomous optimization of intelligent construction operation processes. The above studies show that the combination of BIM and various intelligent optimization algorithms has achieved rich results in structural scheme design, construction process scheduling, component layout, and construction robot control, but the research objects are mostly concentrated on design, planning, and construction levels, and have not fully focused on the in-depth analysis and monitoring algorithm optimization of structural performance monitoring data itself.

For intelligent detection and monitoring of engineering structures, Wang [9] proposed a structural intelligent detection and monitoring method based on particle swarm optimization algorithm, improving the accuracy and stability of monitoring results by optimizing the parameters of feature extraction or classification models, indicating that swarm intelligence optimization has a good application prospect in the field of structural monitoring. However, existing work still has several shortcomings: first, multi-source monitoring data is often simplified and lacks a systematic framework for integrated modeling with structural topology and construction conditions information; second, state assessment models often focus on a certain type of algorithm, lacking the joint description of spatiotemporal coupling features and performance degradation processes; third, at the optimization level, most studies only start from design or a single performance indicator, and rarely consider multiple objective engineering constraints such as prediction accuracy, robustness, real-time performance, and monitoring configuration costs. In contrast, in the intelligent construction scenario, this paper integrates the preprocessing and feature construction of multi-source structural performance monitoring data, time series modeling and state assessment, and optimization algorithms and parameter optimization strategies for engineering constraints, aiming to address the deficiencies in the "monitoring data analysis - state assessment - optimization algorithm" loop of existing research.

3 Intelligent Construction of Building Structure Performance Monitoring Data Analysis and Optimization Algorithms

3.1 Preprocessing and Feature Construction Methods for Multi-source Structural Monitoring Data in Intelligent Construction Environments

In intelligent construction scenarios, building structure performance monitoring often relies on a large number of distributed sensor nodes, BIM models, and on-site construction and operation management systems, forming a typical "engineering structure + Internet of Things + computing platform" integrated data environment. To provide high-quality input for subsequent time series modeling and optimization algorithms, a unified preprocessing and feature construction process for multi-source heterogeneous monitoring data needs to be constructed on the computer platform. This paper divides the preprocessing of multi-source monitoring data into several steps: data unified encoding and storage, temporal alignment and missing data repair, noise suppression and anomaly detection, as well as multi-scale performance feature construction and structural topology embedding.

(1) Structure of Unified Encoding and Storage of Multi-source Monitoring Data The monitoring system usually consists of various types of sensors such as accelerometers, displacement meters, strain gauges, and thermometers, with significant differences in sampling frequency and data format. In this paper, a unified "sensor - component - floor - structure" hierarchical coding system is constructed on the computer end, and the monitoring data is organized into a multi-dimensional time series data table with timestamps as the primary key. The original observation of the i-th sensor at time t is denoted as $x_i(t)$, and its storage structure in the database can be abstracted as:

$$d_i(t) = (id_i, loc_i, type_i, t, x_i(t)) \tag{1}$$

Here, "id_i" represents the sensor number, "loci" is the component and floor coordinate of the sensor in the BIM model, and "type_i" is the type of the monitored physical quantity. By combining the relational database and the time-series database, rapid query and batch reading of monitoring data can be realized in the background, providing support for subsequent parallel computing and sliding window feature extraction. Table 1 presents the multi-source structural monitoring data configuration in the intelligent construction scenario.

Table 1: Multi-source structural monitoring data in the intelligent construction scenario

Sensor Number	Type	Monitoring Physical Quantity	Sampling Frequency / Hz	Corresponding Component
S01	Accelerometer	Floor acceleration	100	Center of the third floor floor slab
S02	Displacement meter	Horizontal displacement	20	Top of the 3-story shear wall
S03	Strain gauge	Axial strain	50	The middle part of column C3-1
S04	Thermometer	Concrete temperature	1	The inner side of the basement exterior wall

(2) Spatio-temporal alignment and missing data repair

Due to different sampling frequencies of different sensors and the existence of communication delay, it is necessary to align and resample the multi-source monitoring data.

Let Δt be the unified time step, and resample the time series $x_i(t)$ of sensor i as:

$$x_i^*(k) = \mathcal{R}(x_i(t), k\Delta t) \tag{2}$$

where R(·) represents a linear interpolation or higher-order spline interpolation operator, and k is the time step index. For time steps with missing data, weighted interpolation based on neighborhood samples is adopted:

$$\hat{x}_i^*(k) = \frac{\sum_{j\in\mathcal{N}_k} \omega_{ij}\, x_i^*(j)}{\sum_{j\in\mathcal{N}_k} \omega_{ij}}, \quad \omega_{ij} = \exp(-\lambda|k-j|) \tag{3}$$

where $\mathcal{N}_k$ is the time neighborhood window, and λ is the attenuation coefficient. This form can be implemented in the computer as a convolution operation on the time series array, with good parallelism.

In terms of spatial alignment, this paper maps the component nodes in the BIM model to the nodes v in the graph structure, and associates the sensor data with the corresponding nodes through the mapping function ϕ, achieving consistency between the monitoring data and the structural topology:

$$v = \phi(\mathrm{loc}_i), \quad x_v(t) = \{x_i(t) \mid \phi(\mathrm{loc}_i) = v\} \tag{4}$$

(3) Noise suppression and outlier detection

Field monitoring data inevitably contains sensor drift, environmental interference, and communication noise. This paper processes it using a combination of "coarse-grained filtering + fine-grained anomaly detection". For each sensor time series, first perform band-pass filtering to remove high-frequency noise and low-frequency drift:

$$\tilde{x}_i^*(k) = \mathcal{F}_{\mathrm{b}p}(\tilde{x}_i^*(k); f_{\mathrm{m}in}, f_{\mathrm{m}ax}) \tag{5}$$

Here, $\mathcal{F}_{\mathrm{bp}}(\cdot)$ is a digital band-pass filtering operator, and $\mathrm{f_{min}}, \mathrm{f_{max}}$ are the passband frequencies.

Subsequently, z-score is used for anomaly detection within the sliding window. The mean $\mu_i^{(w)}$ and standard deviation $\sigma_i^{(w)}$ are calculated for the samples in the window w, and the anomaly score is:

$$z_i^{(w)}(k) = \frac{\tilde{x}_i^*(k) - \mu_i^{(w)}}{\sigma_i^{(w)} + \varepsilon} \tag{6}$$

When $|z_i^{(w)}(k)| > \tau$, the corresponding point is marked as an anomaly, and it is smoothed and replaced by combining adjacent time points. This process can be efficiently implemented on CPU/GPU through matrix vectorization operations, meeting the real-time requirements of large-scale online monitoring in intelligent construction scenarios.

To consider the online health status of the sensors, this paper also introduces a simple reliability weight w_i:

$$w_i = \sigma(\gamma_1 r_i - \gamma_2 n_i) \tag{7}$$

where r_i represents the online rate of the sensor, n_i is the proportion of abnormal points, γ1, γ2 are weight parameters, and σ(·) is the Sigmoid function. This weight will be used as an important coefficient in the subsequent feature fusion.

(4) Construction of multi-scale features for structural performance and structural topology embedding

After the preprocessing is completed, features that can sensitively reflect the evolution of structural performance need to be extracted from the multi-source monitoring data. In this paper, on the computer platform, the sliding window strategy is adopted to construct multi-scale features related to time domain, frequency domain and operating conditions for each monitoring point. For the preprocessed signal of sensor i within the window w, the time domain feature vector is constructed as follows:

$$f_{i,\mathrm{time}}^{(w)} = \left[\mu_i^{(w)}, \sigma_i^{(w)}, \mathrm{RMS}_i^{(w)}, \mathrm{Skew}_i^{(w)}, \mathrm{Kurt}_i^{(w)}\right] \tag{8}$$

The frequency domain features are obtained through the Fast Fourier Transform (FFT):

$$X_i^{(w)}(f) = \mathrm{FFT}(\tilde{x}_i^*(k)),$$
$$\mathbf{f}_{i,\mathrm{freq}}^{(w)} = [E_{\mathrm{low}}, E_{\mathrm{mid}}, E_{\mathrm{high}}, f_{\mathrm{dom}}] \tag{9}$$

Here, E_{low}, E_{mid}, E_{high} represent the energy of different frequency bands, and f_{dom} is the main frequency.

Combining the reliability weights of the sensors, the multi-sensor features belonging to the same component node v are weighted and fused:

$$h_v^{(w)} = \frac{\sum_{i\in\mathcal{S}(v)} w_i \left[f_{i,\mathrm{time}}^{(w)}, f_{i,\mathrm{freq}}^{(w)}\right]}{\sum_{i\in\mathcal{S}(v)} w_i} \tag{10}$$

Here, S(v) represents the set of sensors attached to node v. To explicitly depict the structural topology, this paper uses the adjacency matrix A to represent the connection relationships between components, and obtains the enhanced topological features through a single neighborhood aggregation:

$$\tilde{h}_v^{(w)} = \alpha h_v^{(w)} + (1-\alpha) \sum_{u\in N(v)} a_{vu}\, h_u^{(w)} \tag{11}$$

where N(v) is the neighborhood of node v, avu is the normalized adjacency weight, and α is the balance coefficient between self-information and neighborhood information.

Finally, a structural performance monitoring feature tensor for the time window w is formed in the computer memory:

$$\mathbf{F}^{(w)} = \left\{\tilde{\mathbf{h}}_v^{(w)}, \mathbf{c}^{(w)}, \mathbf{e}^{(w)}\right\}_{v\in\mathcal{V}} \tag{12}$$

Here, $\mathbf{c}^{(w)}$ represents the construction stage and condition code, $\mathbf{e}^{(w)}$ represents the environmental factors (temperature, humidity, wind speed, etc.) characteristics, and V represents the set of structural nodes. This tensor can be directly input into the subsequent time series modeling and state evaluation network through tensor operations and batch processing interface. Table 2 summarizes the structural performance monitoring feature system constructed in this paper.

Table 2: Overview of the Structural Performance Monitoring Feature System

Feature category	Example of specific indicators	Physical meaning
Time-domain features	Mean, standard deviation, RMS, skewness, kurtosis	Reflect the amplitude and waveform shape of the response
Frequency-domain features	Energy of each frequency band, dominant frequency, frequency band energy ratio	Reflect the stiffness change and modal frequency drift
Topological features	Neighborhood aggregated response, inter-layer difference, component combination index	Reflect the coordination between components and the coordination of inter-layer deformation
Condition features	Construction stage code, load condition label	Distinguish different construction/operation states
Environmental features	Temperature, humidity, wind speed, etc. environmental quantities	Represent the influence of the environment on the structural response

Based on the above preprocessing and feature construction process, this paper has achieved the conversion of multi-source structural monitoring data into a unified and high-information-density feature representation in the intelligent construction scenario. While ensuring computational efficiency, it enhances the sensitivity of the features to structural performance degradation and abnormal behaviors, providing a reliable data basis for the subsequent 3.2 section's time series modeling and state evaluation algorithms. Figure 1 gives an overall flow diagram of the preprocessing and feature construction of multi-source structural monitoring data, which can be directly used as a reference for the division of software modules in the computer system during engineering implementation.

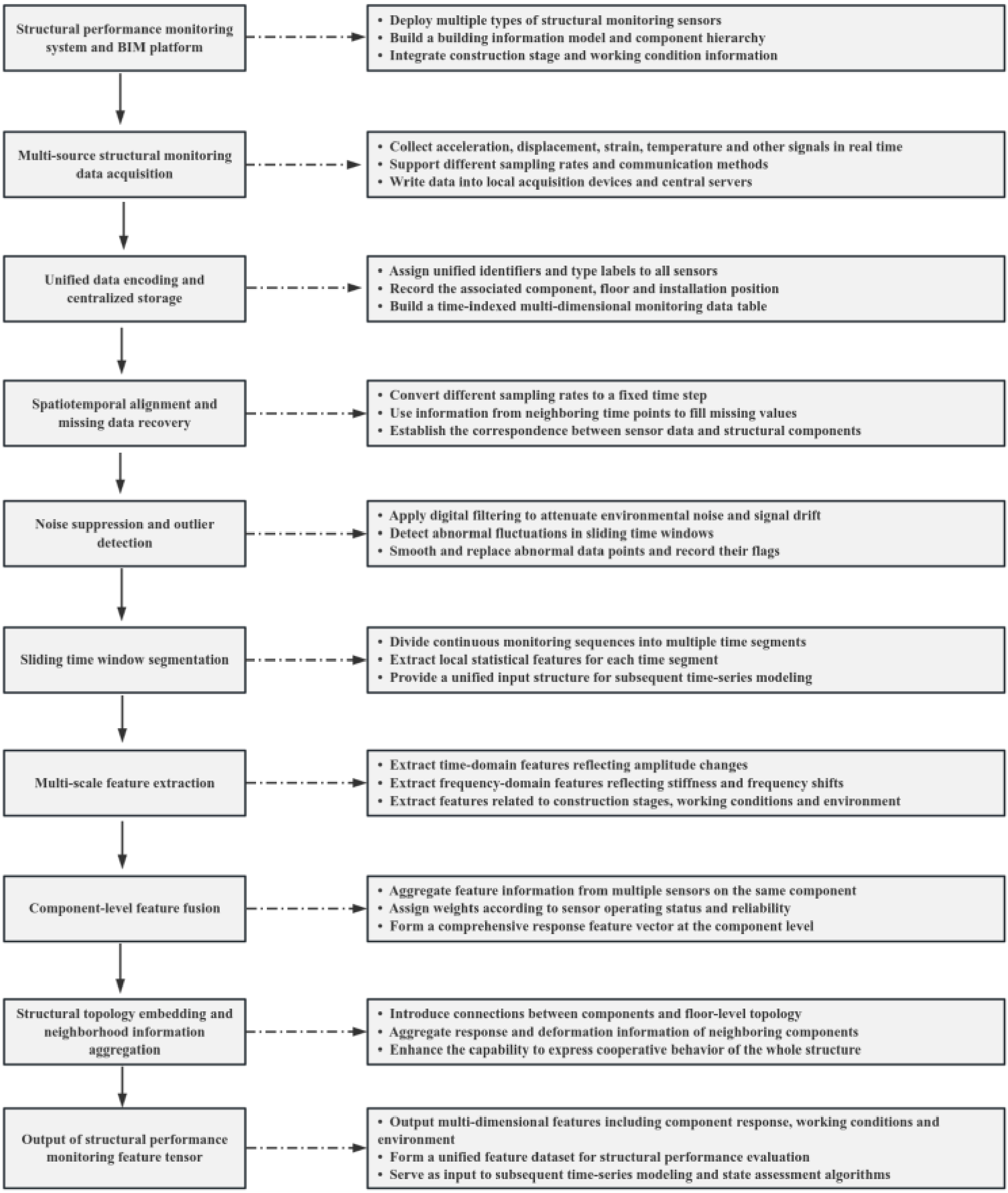

Figure 1: Flowchart of Preprocessing and Feature Construction for Multi-source Structural Monitoring Data

3.2 Design of Time Series Modeling and State Evaluation Algorithms for Building Structure Performance Monitoring Data

After completing the preprocessing and feature construction of multi-source monitoring data in 3.1, the response of the building structure within a given time window has been encoded as a high-dimensional feature tensor with spatial semantics and condition information. To depict the evolution process of structural performance over time and implement an executable state evaluation algorithm on the computer platform, this section constructs a time series modeling and state evaluation framework for building structure performance monitoring data. This framework consists of components such as time series input organization, structure-aware bidirectional encoding, multi-scale attention mechanism, health index construction and state level determination, as well as loss function and training strategy. The overall process can be illustrated as shown in Figure 2.

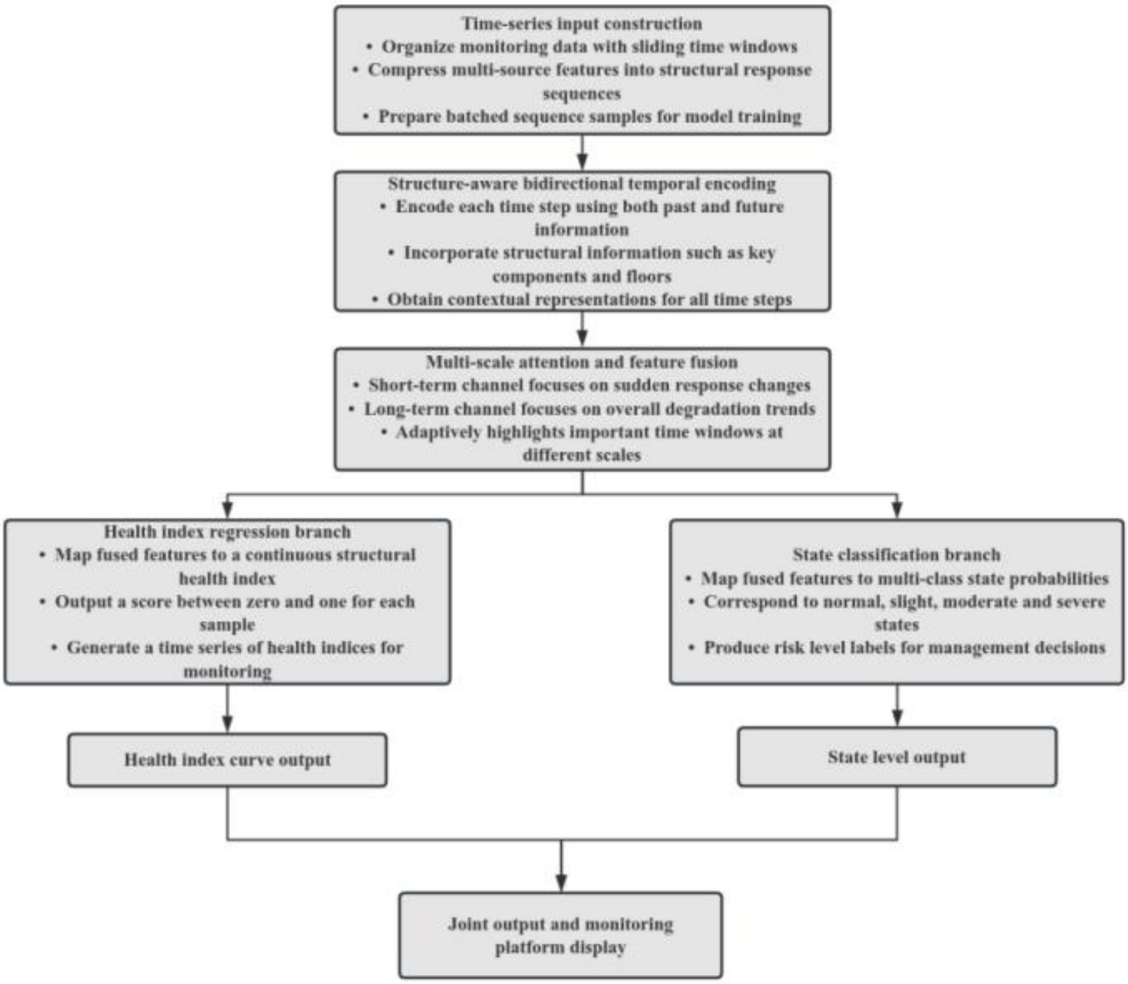

Figure 2: Schematic diagram of the framework for time series modeling and state assessment algorithm for building structure performance monitoring data

(1) Time series input organization and sample construction

Considering that the monitoring process is divided into several adjacent time windows, a snapshot of the structural response is defined for each window. To capture the performance evolution trend, in this paper, a time series sample of length T is constructed in the computer in a sliding manner. Let the input sequence of the nth sample be:

$$\mathcal{S}^{(n)} = \{\mathbf{u}_1^{(n)}, \mathbf{u}_2^{(n)}, \dots, \mathbf{u}_T^{(n)}\} \tag{13}$$

Among them, $\mathrm{u}_{\mathrm{T}}^{(\mathrm{n})}$ is the feature vector obtained by summarizing the entire structure in the t-th time window, including component response features, working condition encoding, and environmental variables. To balance spatial information and computational efficiency, this paper adopts the "structural node pooling" method, aggregating the node-level features at the floor or component group level:

$$u_t^{(n)} = \Psi(\{\tilde{h}_{v,t}\}_{v\in\mathcal{V}}) \tag{14}$$

where $\tilde{h}_{v,t}$ is the topological enhanced feature of node v at time t, and $\Psi(\cdot)$ is a piecewise statistical aggregation operator grouped by floor or component function (such as taking the average for each floor, taking the extreme value for key components, etc.). Through the above processing, while retaining the main spatial differences, the high-dimensional feature tensor can be compressed into a fixed-dimensional time series vector sequence, facilitating subsequent model batch parallel training on the GPU.

(2) Structure-aware bidirectional temporal encoding

To simultaneously utilize historical information and future segments to constrain the current state, this paper builds a structure-aware bidirectional temporal encoding module on the computer side. Let the hidden states of the forward and backward encodings be and , and the update relationship is abstracted as:

$$\mathbf{p}_t^{(n)} = \mathcal{G}_{\mathrm{f}}(\mathbf{p}_{t-1}^{(n)}, \mathbf{u}_t^{(n)}, \mathbf{r}_t^{(n)}) \tag{15}$$

$$\mathbf{q}_t^{(n)} = \mathcal{G}_b\left(\mathbf{q}_{t+1}^{(n)}, \mathbf{u}_t^{(n)}, \mathbf{r}_t^{(n)}\right) \tag{16}$$

Here, $\mathcal{G}_{\mathrm{f}}(\cdot)$ and $\mathcal{G}_{\mathrm{b}}(\cdot)$ represent the forward and backward nonlinear state update units respectively. They can be implemented using long short-term memory units, gated recurrent units, or lightweight gated feedforward modules. $r_t^{(n)}$ is a constraint vector related to the structural topology, such as representing floor shear distribution or component importance weights. By explicitly introducing $\mathbf{r}_t^{(n)}$ in the update function, the model pays more attention to key components and vulnerable floors while modeling time.

For each time step, the forward and backward hidden states are concatenated to obtain the context representation:

$$\mathbf{h}_t^{(n)} = \left[\mathbf{p}_t^{(n)}, \mathbf{q}_t^{(n)}\right] \tag{17}$$

This representation encodes the immediate response characteristics of the structure at the current moment, as well as the constraint information of the past and future windows regarding the state. It provides a foundation for subsequent attention aggregation and health assessment.

(3) Multi-scale Attention Mechanism and Health Index Construction

The evolution of structural performance typically exhibits the characteristic of "slow change superimposed with sudden disturbances". A single time scale is insufficient to balance the long-term degradation trend and the short-term anomalies. Therefore, this paper constructs a multi-scale attention mechanism to adaptively weight different time-scale key windows. For a given sample n, define two attention channels, whose scoring functions are:

$$s_{short,t}^{(n)} = \eta_{short}^{\top} \tanh(\mathbf{W}_{short}\mathbf{h}_t^{(n)} + \mathbf{b}_{short}) \tag{18}$$

$$s_{\mathrm{long},t}^{(n)} = \eta_{\mathrm{long}}^{\top} \tanh(\mathbf{W}_{\mathrm{long}}\mathbf{h}_t^{(n)} + \mathbf{b}_{long}) \tag{19}$$

where $\eta_{\mathrm{short}}, \eta_{\mathrm{long}}, W_{\mathrm{short}}, W_{\mathrm{long}}, b_{\mathrm{short}}, b_{\mathrm{long}}$ are learnable parameters. After normalizing the scores of the two channels, the attention weights are obtained:

$$\alpha_{\mathrm{short},t}^{(n)} = \frac{\exp(s_{\mathrm{short},t}^{(n)})}{\sum_{j=1}^{T}\exp(s_{\mathrm{short},j}^{(n)})},\quad \alpha_{\mathrm{long},t}^{(n)} = \frac{\exp(s_{\mathrm{long},t}^{(n)})}{\sum_{j=1}^{T}\exp(s_{\mathrm{long},j}^{(n)})}. \tag{20}$$

Based on this, two structural response feature representations of short-term and long-term are constructed:

$$z_{\mathrm{short}}^{(n)} = \sum_{t=1}^{T} \alpha_{\mathrm{short},t}^{(n)} h_t^{(n)}, \quad z_{\mathrm{long}}^{(n)} = \sum_{t=1}^{T} \alpha_{\mathrm{long},t}^{(n)} h_t^{(n)} \tag{21}$$

The comprehensive representation is obtained through linear combination:

$$\mathbf{z}^{(n)} = \beta \mathbf{z}_{short}^{(n)} + (1-\beta)\mathbf{z}_{long}^{(n)} \tag{22}$$

where β is a learnable or manually set balance coefficient used to control the proportion of the model's attention to short-term anomalies and long-term trends.

The health index is represented in a normalized scalar form, mapping the overall structural state to the interval [0,1]:

$$H^{(n)} = \sigma(\mathbf{w}_H^{\mathrm{T}} \mathbf{z}^{(n)} + b_H) \tag{23}$$

where σ(·) is the activation function, and w_H, b_H are the parameters to be learned. The health index close to 1 indicates that the structure is in a safe state, while close to 0 indicates that the structure has a significant potential risk.

To facilitate engineering applications, this paper further divides the health index into several performance levels, corresponding to different state interpretations, as shown in Table 3.

Table 3: Classification of Structural Performance States and Engineering Meanings

Level	Health Degree Range	Engineering State Description
0	0.80 and above	Overall performance is good, the structure is in a normal state
1	0.60–0.80	Minor performance degradation, monitoring is recommended
2	0.40–0.60	Moderate degradation, special inspection and assessment are required
3	0.40 and below	Performance is significantly deteriorated, reinforcement measures should be taken promptly

In implementation, the threshold values of the levels can be adjusted according to the safety levels and specification requirements of different engineering projects. After model training, the health index and corresponding levels can be automatically output, providing intuitive alarm signals for the monitoring platform.

(4) State Evaluation Output and Classification Branch Design

In addition to continuous health degree indicators, engineering management usually also pays attention to whether the structure is in a certain specific state (such as "normal / abnormal", "whether it exceeds the warning line", etc.). Therefore, in addition to the continuous health degree regression branch, this paper adds a state classification branch to map the comprehensive representation z(n) to a multi-class state probability vector:

$$\mathbf{p}^{(n)} = \mathrm{softmax}\left(\mathbf{W}_S \mathbf{z}^{(n)} + \mathbf{b}_S\right) \tag{24}$$

Here, W_S and b_S are parameters of the state classification layer, and the components of $\mathbf{p}^{(n)}$ correspond to the prediction probabilities of different state levels in Table 3. The final state can be determined by the maximum probability criterion, or conservative decision rules can be set based on safety requirements, such as using stricter thresholds for high-risk levels.

This dual-output structure, on the one hand, provides a continuously adjustable quantitative health indicator for the monitoring platform, facilitating trend analysis and life prediction. On the other hand, it provides discrete state labels for on-site managers, facilitating rapid decision-making and linkage control. Both can be visually displayed in the form of line graphs and color markings in the computer system interface.

(5) Loss Function and Training Strategy

To ensure the accuracy of state discrimination while maintaining the smoothness and monotonicity of the health curve, this paper constructs a composite loss function that includes regression, classification, and temporal constraints. Let $\widehat{H}^{(n)}$ be the health degree label given in the training set, and $\hat{\mathbf{y}}^{(n)}$ be the one-hot encoding of the state level label. Then, the single-sample loss can be written as:

$$\mathcal{L}^{(n)} = \lambda_1\left(H^{(n)} - \widehat{H}^{(n)}\right)^2 + \lambda_2\left(-\hat{\mathbf{y}}^{(n)}\right)^{\mathsf{T}} \log \mathbf{p}^{(n)} + \lambda_3 \Omega^{(n)} \tag{25}$$

where the first two terms are the health degree regression error and the cross-entropy loss of state classification, λ1, λ2, λ3 are weight coefficients, and Ω(n) is the term for temporal smoothing and monotonicity constraints.

Considering that the degradation of structural performance usually presents a smooth change over time and develops in an unfavorable direction over the long term, this paper adopts the penalty form of the difference in health degrees between adjacent samples:

$$\Omega^{(n)} = \frac{1}{T-1}\sum_{t=1}^{T-1}\left[\begin{array}{c} \omega_{smooth}\left(H_{t+1}^{(n)} - H_t^{(n)}\right)^2 + \\ \omega_{trend}\max\left(0, H_t^{(n)} - H_{t+1}^{(n)} - \delta\right) \end{array}\right] \tag{26}$$

where $H_t^{(n)}$ is the estimated health degree of sample n at time step t, ω_{smooth} and ω_{trend} are the smoothing and trend weights, and δ is the allowable small fluctuation threshold. The first term encourages smooth changes in health degrees between adjacent samples, and the second term penalizes "reverse jumps" that are opposite to the expected degradation trend and have a large amplitude, thereby weakening short-term abnormal oscillations caused by noise, making the model output more in line with engineering experience.

In terms of the training strategy, this paper adopts mini-batch stochastic gradient descent and adaptive learning rate optimization algorithms for model training on computer clusters or single-machine GPUs. To improve generalization ability, data augmentation methods such as monitoring noise perturbation and condition masking are introduced during training, enabling the model to still provide stable state assessment results even when facing missing measurements and abnormal conditions. The main parameter settings can be summarized in Table 4 to facilitate the reproduction of the experimental process in the subsequent sections.

Table 4: Example of Main Parameter Settings for Time Series Modeling and State Assessment Model

Parameter Name	Example Value	Explanation
Time Window Length	32	Number of time steps per sample
Forward and Backward Hidden Dimensions	64	Dimension of bidirectional time series encoding hidden state
Short-Term Attention Channel Weight	Pre-set or Adaptive	Controls the degree of attention to sudden responses
Long-Term Attention Channel Weight	Pre-set or Adaptive	Controls the degree of attention to degradation trends
Smoothing Constraint Weight	0.1	Adjustment of the smoothness of the health degree curve
Trend Constraint Weight	0.05	Strength of suppressing unreasonable reverse jumps

Through the design of the above time series modeling and state assessment algorithm, the monitoring data of building structure performance is transformed into a health degree curve and state level sequence with clear engineering meaning on the computer end. Compared with methods that rely solely on single-time indicators or static classification models, this framework can better capture the evolution process of structural performance and the impact of key conditions on the state, providing an algorithmic basis for the robustness and generalization ability analysis in Chapter 4.

3.3 Optimized Algorithms and Model Parameter Optimization Strategies for Structural Performance Monitoring

After completing the construction of multi-source monitoring features and the design of the time series state assessment model, the performance of the model largely depends on a series of key hyperparameters and monitoring configurations, such as the length of the time window, the bidirectional encoding hidden dimension, the attention channel weights, the smoothing and trend constraint coefficients, and the set of sensors involved in the modeling. If only relying on experience or simple grid search, it is often difficult to achieve a reasonable balance between prediction accuracy, output stability, computational cost, and monitoring cost. Therefore, this paper constructs a multi-objective optimization framework for the structural performance monitoring scenario, uniformly encoding the model parameters and some monitoring configurations as a vector to be optimized, and achieving automatic optimization through the improvement of swarm intelligence optimization algorithms.

(1) Optimization variable encoding and search space construction

All the continuous and discrete variables to be optimized are uniformly regarded as a decision vector of length D. The decision variable of the dth dimension is denoted as χd, and the overall representation is:

$$\chi = [\chi_1, \chi_2, \dots, \chi_D]^t \tag{27}$$

In the evolutionary algorithm, normalized real number encoding is adopted, and the "gene value" of each dimension gd is restricted to the interval [0,1], and the corresponding actual physical quantity is obtained through linear mapping:

$$\chi_d = a_d + (b_d - a_d) g_d, \quad d = 1,2,\dots,D \tag{28}$$

Here, a_d and b_d represent the lower and upper bounds allowed for the d-th variable. For discrete variables (such as time window length, hidden dimension, allowed number of sensors, etc.), after mapping, they are rounded and projected onto the valid set. In this way, it is convenient to perform vectorized operations on the computer and ensure that the search process always remains within the preset engineering constraints. Table 5 presents examples of typical optimization variables and their value ranges in this study, facilitating the reproduction of subsequent experimental chapters.

Table 5: Optimization Variables and Value Ranges for Structural Performance Monitoring Model

Optimization Variable	Meaning Description	Encoding Type	Value Range
Time Window Length	Number of time steps in each sample	Integer Type	16–64
Hidden State Dimension	Length of the hidden vector of the bidirectional temporal encoding unit	Integer Type	32–128
Short-Term Attention Weight	Proportion of the short-term channel in feature fusion	Real Type	0.2–0.8
Smoothing Constraint Coefficient	Strength of the smoothness constraint of the health curve	Real Type	0.00–0.20
Trend Constraint Coefficient	Strength of the degradation trend constraint	Real Type	0.00–0.10
Allowed Number of Sensors	Upper limit of the number of monitoring points involved in modeling	Integer Type	50–120

(2) Design of Multi-Objective Optimization Indicators

For intelligent construction scenarios, model optimization should not only focus on the accuracy of structural performance status assessment, but also take into account the smoothness and reliability of the output curve, the robustness to noise and operational disturbances, as well as the real-time and cost constraints given the available computing resources and sensor configuration conditions. This paper constructs three relatively independent but interrelated objective functions.

Accuracy Objective Function reflects the overall error of the health degree and state grade prediction. It combines the normalized absolute error on the validation set and the state misjudgment rate through weighted addition:

$$\Phi_1(\boldsymbol{x}) = \frac{1}{N_{val}} \sum_{n=1}^{N_{val}} \theta_{\mathrm{h}} \frac{H^{(n)}(\boldsymbol{x}) - H_{ref}^{(n)}}{\max(\varepsilon, H_{ref}^{(n)})} + \theta_s \xi^{(n)}(\boldsymbol{x}) \tag{29}$$

where $H^{(n)}(\boldsymbol{x})$ is the predicted health degree of the current parameter configuration for the nth sample, $\mathrm{H}_{\mathrm{ref}}^{(\mathrm{n})}$ is the reference calibration value, $\xi^{(n)}(\boldsymbol{x})$ represents the indicator of whether the corresponding sample's state grade is misjudged, θ_h,θ_s are weight coefficients, and ε is a small constant to prevent the denominator from being zero.

Robustness Objective Function is used to characterize the smoothness and stability of the health degree sequence under different noise scenarios and operating conditions. Let the m-th group of scenarios contain Tm time steps, and the corresponding health degree sequence be $H_{m_1}(\chi), \dots, H_{m,T\mathrm{m}}(\chi)$. The curvature of the curve is measured by the average absolute value of the second-order difference:

$$\Phi_2(\chi) = \frac{1}{M}\sum_{m=1}^{M}\frac{1}{T_m - 2}\sum_{t=2}^{T_m-1} | H_{m,t+1}(\chi) - 2H_{m,t}(\chi) + H_{m,t-1}(\chi)| \tag{30}$$

The smaller this indicator is, the smoother the health degree curve is, less sensitive to local abnormal points, and more in line with the engineering characteristic of slow degradation of structural performance.

Cost Objective Function focuses on the computing time for model deployment and the cost of monitoring configuration. Let Ctime(χ) be the average time consumed for a single forward inference, and Csens(χ) be the current number of participating sensors or their weight sum. The comprehensive cost objective is defined as:

$$\Phi_3(\boldsymbol{x}) = \kappa_t \, C_{time}(\boldsymbol{x}) + \kappa_c \, C_{sens}(\boldsymbol{x}) \tag{31}$$

where κt,κc are the weight coefficients for time consumption and monitoring cost, which can be set according to engineering budget and real-time requirements.

To facilitate the joint processing of objectives of different scales, this paper adopts an online normalization strategy, mapping each objective function to the interval [0,1]:

$$\bar{\Phi}_j(\chi) = \frac{\Phi_j(\chi) - \Phi_j^{\min}}{\Phi_j^{\max} - \Phi_j^{\min} + \epsilon_j}, \quad j = 1,2,3 \tag{32}$$

Here, $\Phi_j^{\min}$ and $\Phi_j^{\max}$ represent the minimum and maximum observed values of the target within the current population, respectively, and ϵ_j is a stabilizing term to prevent the denominator from being zero. According to actual needs, the comprehensive fitness can be constructed in a weighted summation form, or non-dominated sorting can be combined with Pareto sorting and crowding distance for non-dominated ranking, to diversely retain different trade-off solutions.

(3) Multi-objective Optimization Algorithm Based on Improved Particle Swarm

In the optimization solution strategy, this paper adopts the improved particle swarm algorithm as the core search engine. On the one hand, the particle swarm algorithm has a simple structure and is easy to be implemented in computer clusters and graphics processors in parallel; on the other hand, by introducing adaptive inertia weight and perturbation mechanism, it can effectively balance the global exploration and local development capabilities.

Let the current position of the i-th particle in the population be χi(k), and its velocity be vi(k), with the iteration number being k. To balance the early global search and the later local convergence, the inertia weight adopts a nonlinear decaying form with respect to the iteration:

$$\omega(k) = \omega_{\min} + \frac{\omega_{\max} - \omega_{\min}}{1 + \exp(\alpha(k - k_0))} \tag{33}$$

where ω_{max} and ω_{min} are the initial and final inertia weights, α controls the decay rate, and k0 is the turning point position.

The particle velocity and position are updated as follows:

$$\boldsymbol{v}_i(k+1) = \omega(k)\boldsymbol{v}_i(k) + c_1 r_1(\boldsymbol{p}_i - \chi_i(k)) + c_2 r_2(\boldsymbol{g}(k) - \chi_i(k)) \tag{34}$$

$$\chi_i(k+1) = \chi_i(k) + \lambda v_i(k+1) \tag{35}$$

where $\boldsymbol{p}_i$ is the historical optimal position of the particle itself, $\boldsymbol{g}(k)$ is the representative and excellent solution of the current population (which can be randomly selected from the non-dominated solution set), c_1 and c_2 are learning factors, r_1 and r_2 are uniformly distributed random numbers, and λ is the step size factor.

To avoid premature convergence of particles to a local region, this paper introduces a Gaussian perturbation type mutation operator for some individuals:

$$\chi_i'(k+1) = \chi_i(k+1) + \sigma(k)\xi_i \tag{36}$$

where ξi is an independent standard normal random vector in each dimension, $\sigma(k)$ is a gradually decreasing perturbation scale function with respect to the iteration, ensuring sufficient exploration in the early stage and fine adjustment in the later stage. The mutated individuals are re-projected to the legal parameter space and participate in multi-objective evaluation and non-dominated sorting. The multi-objective optimization process for structural performance monitoring is shown in Figure 3.

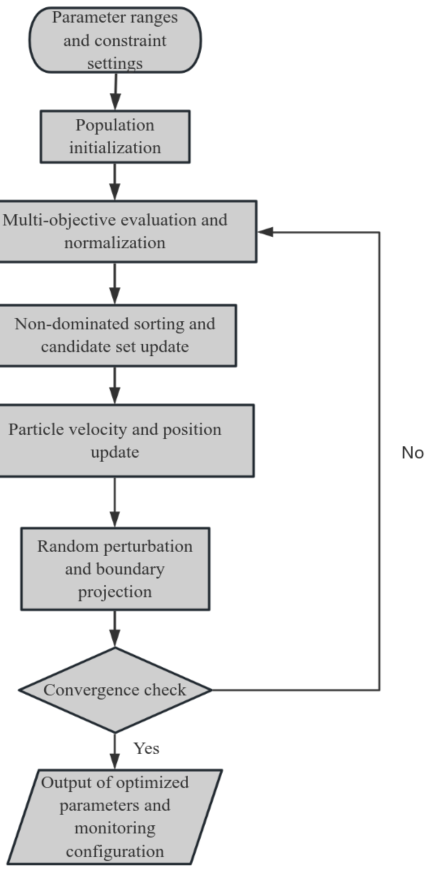

Figure 3: Flowchart of Multi-objective Parameter Optimization for Structural Performance Monitoring

4 Experimental Design and Result Analysis

4.1 Experimental Scheme and Dataset Description

To verify the effectiveness and applicability of the proposed data analysis and optimization algorithm for building structure performance monitoring in intelligent construction scenarios, this paper constructs three representative test datasets based on actual engineering monitoring data and simulation extended data, covering different structural types such as high-rise civil buildings, shear wall-frame hybrid structures, and industrial plants, while also considering various working conditions such as construction later stage, normal operation, strong wind, and equipment vibration. The overall experimental scheme includes dataset construction and division, comparison method setting, and evaluation index system design. This section focuses on the dataset and working condition configuration, and the subsequent subsections will discuss the results comparison and robustness analysis from the perspectives of result comparison and robustness analysis.

In terms of dataset construction, the S1 dataset selects continuous monitoring data of a high-rise reinforced concrete frame structure under normal operation and strong wind conditions, with sensors mainly placed at the center of the floor slab, frame columns, and top of the shear wall; the S2 dataset comes from the monitoring records of a shear wall-frame hybrid structure during the construction later stage and load test stage, highlighting the performance changes during the transition from construction state to operation state of the structure; the S3 dataset comes from a steel structure industrial plant, with monitoring objects including roof components and main equipment foundations, able to reflect the influence of equipment vibration on the structure response. Each dataset is processed uniformly using the pre-processing and feature construction process described earlier, and is divided into training set, validation set, and test set in chronological order to avoid information leakage.

Table 6 gives the basic information and time window scale of the three datasets. From the table, it can be seen that the three datasets have significant differences in structural type, number of floors, monitoring duration, and number of monitoring points, which are conducive to evaluating the generalization ability of the algorithm in different structures and working conditions scenarios; at the same time, the overall scale of training, validation, and test time windows is in the tens of thousands, providing sufficient sample support for the state assessment model and optimization algorithm.

Table 6: Statistics of Monitoring Datasets and Experimental Working Conditions

Dataset Number	Structural Type	Number of Floors	Monitoring Duration (days)	Main Working Condition Stage	Monitoring Point Number	Time Window Scale (Training / Validation / Test)
S1	Reinforced Concrete Frame Structure	18	60	Normal Operation, Strong Wind Conditions	64	25000 / 5000 / 5000
S2	Shear Wall-Frame Hybrid Structure	22	45	Construction Later Stage, Structural Load Test	72	20000 / 4000 / 4000
S3	Steel Structure Industrial Plant	8	30	Normal Operation, Equipment Vibration Conditions	48	15000 / 3000 / 3000

Based on this, this paper sets multiple comparison methods on each dataset and adopts a unified training and evaluation process: in the training stage, the training set is used to learn model parameters and optimization algorithm configuration; in the validation stage, it is used to adjust hyperparameters and early stopping judgment; in the test stage, it evaluates the health prediction error, state classification accuracy, and inference time consumption on data that has not participated in training. Such an experimental scheme not only ensures the objectivity and reproducibility of the results, but also provides a unified platform for fair comparison and robustness analysis of different methods in the future.

4.2 Experimental Results and Comparative Evaluation of Monitoring Analysis and Optimization Algorithms

To comprehensively evaluate the effectiveness of the data analysis and optimization algorithm for building structure performance monitoring proposed in this paper, this section compares the differences among threshold discrimination methods, traditional machine learning methods, conventional models, and the method presented in this paper from three aspects: overall index comparison, health degree curve comparison under typical working conditions, and performance in different data set scenarios. The formulas are not provided in Chapter 4, but the algorithm effects are explained through charts and text analysis.

(1) Overall Performance Index Comparison

Under a unified training and testing process, five schemes including threshold discrimination method, random forest method, unidirectional recurrent neural network model, bidirectional recurrent network with single-scale attention model, and the method presented in this paper were selected to compare the health degree prediction error, state classification accuracy rate, macro average F1 value, and inference time on three data sets. To facilitate presentation, the results of each method on the three data sets were weighted averaged and listed in Table 7.

Table 7: Comparison of Overall Structural Performance State Evaluation Results of Different Methods

Method	Health Degree Prediction Error (RMSE)	State Classification Accuracy Rate (%)	Macro Average F1 Value (%)	Per Thousand Window Inference Time (Seconds)
Threshold Discrimination Method	0.142	82.3	78.9	0.8
Random Forest Method	0.118	86.1	83.4	1.4
Unidirectional Recurrent Neural Network Model	0.095	89.7	88.1	1.9
Bidirectional Recurrent Network + Single-scale Attention Model	0.082	91.5	90.2	2.1
The Method of This Paper (Multi-scale Attention + Optimization)	0.074	93.8	92.7	2.4

As can be seen from Table 7, as the models progress from threshold discrimination, random forest, to recurrent neural networks and this method, the health degree prediction error shows a general downward trend, and the state classification accuracy rate and macro average F1 value increase simultaneously. Taking the health degree prediction error as an example, the root mean square error of the threshold discrimination method is approximately 0.142, that of the random forest is 0.118, that of the unidirectional recurrent neural network further drops to 0.095, that of the bidirectional recurrent network with single-scale attention model reaches 0.082, while the method of this paper, after introducing the multi-scale attention mechanism and multi-objective optimization, can further compress the error to 0.074. The state classification accuracy rate and macro average F1 value also show a similar trend: from 82.3% and 78.9% of the threshold discrimination method, to 86.1% and 83.4% of the random forest, to 91.5% and 90.2% of the bidirectional recurrent network with single-scale attention model, and finally reaching 93.8% and 92.7% under the method of this paper. It can be considered that compared with the optimal comparison model, this method improves the accuracy and F1 value by approximately 2 percentage points on average. In terms of inference time, the calculation time per thousand windows of this method is approximately 2.4 seconds, which is slightly increased compared to 2.1 seconds of the bidirectional recurrent network with single-scale attention model, but still within the same order of magnitude compared to the threshold discrimination and random forest methods, and the overall inference overhead can be controlled within minutes or even finer time scales, which can meet the real-time requirements for online structural performance assessment in intelligent construction scenarios.

(2) Comparison of Health Degree Curves under Typical Working Conditions

To visually demonstrate the ability of different methods to depict the evolution process of structural performance, a certain strong wind condition period in the S1 data set was selected, and the health degree curves of the threshold discrimination method, the bidirectional recurrent network with single-scale attention model, and the method presented in this paper were plotted for this period, as shown in Figure 4. The horizontal axis represents the sequence number of time windows, and the vertical axis represents the normalized health degree index, with key moments of significant enhancement and weakening of the strong wind marked.

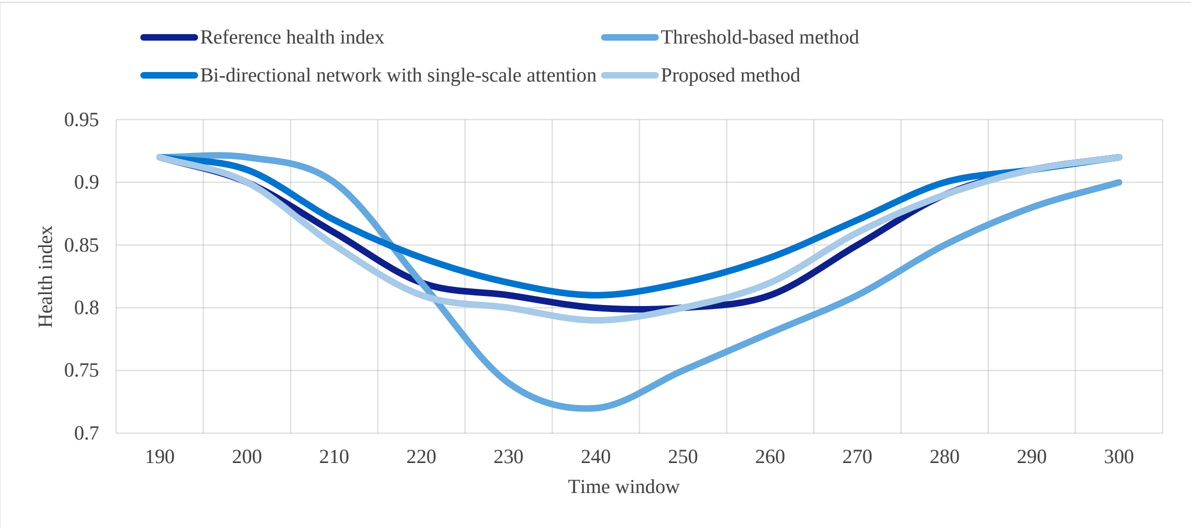

Figure 4: Comparison diagram of health degree curves under typical strong wind conditions for different methods

From Figure 4, it can be observed that within the approximately 200-260 time windows when the strong wind significantly intensified, the reference health degree decreased from about 0.92 to around 0.80, while the curve of the threshold discrimination method lagged about 10 time windows before showing a significant drop, reaching the lowest value of approximately 0.72. Moreover, it fluctuated by about 0.06 up and down multiple times within the 50 time windows after the strong wind ended, easily causing false alarms or missed detections during the recovery phase. The bidirectional cyclic network combined with the single-scale attention model was able to track the changes in health degree in the overall trend relatively well. During the strong wind period, the minimum value was approximately 0.81, which was basically close to the reference curve. However, near some transient disturbance points, there were still one-time local oscillations of about 0.03 to 0.04. In contrast, the health degree curve output by the method in this paper showed a synchronous decrease in the first few time windows after the strong wind began, with the minimum value being approximately 0.79, which was within a deviation of about 0.01 to 0.02 of the reference value. After the strong wind ended, the health degree recovered smoothly within approximately 30 time windows to above 0.90, with the local fluctuation amplitude generally not exceeding 0.02. These results indicate that the method in this paper is more sensitive to the start and end of the strong wind, can timely reflect the phased decline and recovery of the structural performance, and maintains better smoothness over a long period, without over-amplifying isolated abnormal points. The multi-scale attention mechanism and time sequence constraint design achieved a more reasonable compromise between "sensitivity to sudden conditions" and "stability of long-term trends".

(3) Comprehensive analysis under different data sets scenarios

Under different structural types and working condition scenarios, the performance of each method varies. For the dataset S1 of high-rise frame structures, the monitoring duration is relatively long and the working conditions change relatively smoothly. The method in this paper achieved the best results in terms of health degree prediction error and state classification accuracy, and the health degree curve is highly consistent with the subjective assessment trend of engineers, indicating that the algorithm can effectively capture the performance evolution of high-rise structures under wind loads and daily operational conditions.

In the dataset S2 of shear wall-frame hybrid structures, the working conditions at the construction stage and the load test stage switched frequently, and some monitoring points had short-term missing data. Traditional methods were prone to misjudgment near the switching of working conditions, and the one-way cyclic network had large fluctuations in the output near the missing data segments. However, the method in this paper relied on the multi-source features constructed in the early stage and the strategy for missing data repair, as well as the constraints on curve smoothness and robustness in multi-objective optimization, and had more obvious performance advantages in this dataset.

For the dataset S3 of steel structure industrial plants, the vibration components of equipment are complex and the local response is strong, which poses higher requirements for the anti-noise ability of the monitoring model. The experimental results show that although the overall error in S3 dataset is slightly higher than that in S1 and S2, it is still superior to other comparison methods, especially in the periods with frequent equipment start-stop, the health degree curve can remain relatively stable and will not cause a significant change in the state level due to short-term high-frequency vibration. This indicates that the method in this paper has better generalization ability and engineering applicability under different structural types and working condition combinations.

Based on the above comparisons, it can be concluded that the proposed data analysis and optimization algorithm for building structure performance monitoring in this paper outperforms common baseline methods in terms of overall accuracy, health degree curve shape, and cross-scenario performance, providing strong support for subsequent robustness analysis and engineering application effect evaluation (see Section 4.3).

4.3 Analysis of Model Robustness, Generalization Ability and Engineering Application Effect

In the intelligent construction scenario, the structural performance monitoring algorithm needs to maintain a relatively stable assessment ability under complex conditions such as noise enhancement, monitoring point absence, and structural type changes. Therefore, based on the aforementioned three datasets, this paper constructs four typical scenarios: baseline conditions, noise enhancement, monitoring point absence, and cross-structure generalization. A systematic comparison is made between the bidirectional recurrent network with a single-scale attention model and the method proposed in this paper. The prediction errors of health degree and the accuracy of state classification under different interference conditions are shown in Table 8.

Table 8: Comparison of model robustness and generalization performance under different interference conditions

Scenario	Interference type description	Method	Health degree prediction error	State classification accuracy / %
Scenario A Baseline condition	Standard noise level	Bidirectional network + single-scale attention model	0.082	91.5
		This method	0.074	93.8
Scenario B Noise enhancement	Significant increase in sensor noise	Bidirectional network + single-scale attention model	0.113	86.4
		This method	0.092	90.3
Scenario C Monitoring point absence	Randomly missing about 20% of monitoring points	Bidirectional network + single-scale attention model	0.121	84.7
		This method	0.099	88.9
Scenario D Cross-structure generalization	Testing on new structures not involved in training	Bidirectional network + single-scale attention model	0.129	83.6
		This method	0.106	87.4

From Table 8, it can be seen that in the baseline condition, both methods can achieve high assessment accuracy, but the method proposed in this paper is slightly superior to the comparison model in terms of health degree prediction error and state classification accuracy. When the sensor noise significantly increases, the health degree error of the bidirectional model rises from 0.082 to 0.113, and the accuracy drops from 91.5% to 86.4%; the error of this method increases from 0.074 to 0.092, and the accuracy drops from 93.8% to 90.3%, with a significantly smaller decline in accuracy. In the scenario of randomly missing about 20% of monitoring points, the error of the bidirectional model further rises to 0.121, and the accuracy drops to 84.7%, while this method still keeps the error at 0.099 and the accuracy at 88.9%, resulting in a better continuity and stability of the health degree curve. In the cross-structure generalization test, the errors and accuracies of both methods deteriorate, but this method is still superior to the comparison model, indicating that the combination of multi-source feature construction, multi-scale attention, and multi-objective optimization helps improve the model's adaptability to different structural types and combination of conditions.

From an engineering application perspective, under the above different conditions and datasets, the inference time of this method remains at approximately 2–3 seconds per thousand time windows, and it can be deployed on conventional engineering monitoring servers or edge computing nodes to meet the online status update requirements of minutes or even finer time scales. The health degree curves and state level outputs are basically consistent with the subjective judgment of on-site engineers in key conditions such as strong wind, load tests, and equipment vibration, avoiding frequent false alarms of simple threshold methods and outperforming some deep models in overly "sensitive" responses in strong interference scenarios, which is conducive to supporting graded warnings, inspection scheduling, and reinforcement decisions in actual projects. Overall, this method shows good comprehensive balance in noise robustness, cross-structure generalization ability, and engineering usability, providing strong support for its application in larger-scale intelligent construction monitoring systems.

5 Conclusion

This paper focuses on the data analysis and optimization issues of building structure performance monitoring in the intelligent construction environment, and constructs a complete algorithm framework from the preprocessing and feature construction of multi-source monitoring data, time series modeling and state evaluation, to multi-objective optimization and search. Through a unified "sensor - component - floor - structure" hierarchical encoding and spatio-temporal alignment mechanism, combined with noise suppression, anomaly detection and topological enhancement feature fusion, this paper realizes the effective conversion of multi-source heterogeneous monitoring data into high information density feature representation; on this basis, the structural perception bidirectional time series encoding and multi-scale attention mechanism are introduced, jointly outputting continuous health curves and discrete state grades, and through a composite loss including smoothing and trend constraints, the consistency between the output and engineering experience is enhanced; further, the multi-objective optimization strategy of the improved particle swarm is utilized to jointly optimize the model hyperparameters and sensor configuration under the constraints of accuracy, robustness and monitoring cost.

Based on three monitoring data sets covering high-rise frames, shear wall-frame hybrid structures and steel structure workshops, the experimental results show that the proposed method significantly outperforms baseline methods such as threshold discrimination, random forest, unidirectional recurrent network and bidirectional network with single-scale attention: the health prediction error decreases from 0.142 to 0.074, the state classification accuracy increases from 82.3% to 93.8%, and the macro average F1 value increases to 92.7%; in scenarios with enhanced sensor noise and approximately 20% random missing of monitoring points, the error increase and accuracy decrease of this method are significantly smaller than those of the comparison models, and it can still maintain an error of approximately 0.106 and an accuracy of 87.4% on new structures that were not involved in training, while the inference time per thousand time windows is controlled within the 2-3 second range, meeting the requirements of online engineering assessment. Overall, the proposed data analysis and optimization algorithm framework achieves a good balance between accuracy, robustness, generalization ability and engineering usability. In the future, by combining more actual engineering cases and long-term monitoring data, it will be expanded to more structural types and complex conditions, introduce digital twin and online incremental learning mechanisms, and further enhance the application depth and promotion value of the model in the safety monitoring and risk warning of the entire life cycle of structures.

About the Author

Tairan Zhang was born in Enshi, Hubei。P.R. China, in 2001. He obtained a bachelor's degree from South West Jiaotong University in China. I am currently studying at the School of Civil and Environmental Engineering, Nanyang Techonlogical University. My main research direction is CIVIL Engineering

References

[1] Fan C, Ding Y, Liu X, et al. A review of crack research in concrete structures based on data-driven and intelligent algorithms[J]. Structures, 2025, 75: 118298. https://doi.org/10.1016/j.istruc.2025.108800

[2] Li Y, Zhang Y. Computer algorithm optimization of BIM and reinforcement learning in complex building structure construction process optimization under big data environment[J]. Procedia Computer Science, 2025, 261: 262-269. https://doi.org/10.1016/j.procs.2025.04.202.

[3] Huang H, Liu Z, Wang Y, et al. BIM and data-driven multi-objective optimization of asphalt pavement structure combinations[J]. Automation in Construction, 2025, 177: 106348. https://doi.org/10.1016/j.autcon.2025.106348.

[4] Zhang S, Yin P, Wang J, et al. An integrated parametric structural design tool for super high-rise buildings based on Grasshopper and intelligent algorithm[J]. Proceedings of SPIE, 2022.https://doi.org/10.1117/12.2628162.

[5] Li Y. Optimization method of building structure design based on genetic algorithm[J]. Procedia Computer Science, 2025, 262: 1344-1351. https://doi.org/10.1016/j.procs.2025.05.180.

[6] Pham V H S, Dau T D, Nguyen T T. Optimizing floor tile design in residential spaces using nesting algorithm and multi-objective optimization with BIM data[J]. Canadian Journal of Civil Engineering, 2025, 52(4): 267-276. https://doi.org/10.1139/cjce- 2024-0240.

[7] Golmaei S M, Vahidi J, Jamshidi M. Whale algorithm for schedule optimization of construction projects employing building information modeling[J]. Engineering Reports, 2025, 7(3): e70022.https://doi.org/10.1002/eng2.70022.

[8] Jin R. Path planning and control of building robots based on reinforcement learning algorithm in intelligent construction[J]. Procedia Computer Science, 2025, 261: 637-646.https://doi.org/10.1016/j.procs.2025.04.255.

[9] Wang X. Research on intelligent detection and monitoring of engineering structures based on particle swarm optimization algorithm[J]. 2023 International Conference on Telecommunications, Electronics and Informatics (ICTEI), 2023: 55-59. https://doi.org/10.1109/ictei60496.2023.00122.

[10] Son P V H, Khoi L N Q. Optimization of Construction Projects Time-Cost-Quality-

Environment Trade-off Problem Using Adaptive Selection Slime Mold Algorithm[J]. Journal of Soft Computing in Civil Engineering, 2024, 8(1): 107-125. https://doi.org/10.22115/SCCE.2023.390042.1622.

[11] Chen H, Shen Q G, Skibniewski M J, et al. Dynamic prediction and optimization of tunneling parameters with high reliability based on a hybrid intelligent algorithm[J]. Information Fusion, 2025, 114: 102705.https://doi.org/10.1016/j.inffus.2024.102705.

[12] Gao X, Wang J. A Review of Optimization Algorithms Applied to Prefabricated Building Construction[J]. Lecture Notes in Operations Research, 2022: 1102-1113. https://doi.org/10.1007/978-981-19-5256-2_86.

[13] Yin H. Multi-objective optimization analysis of construction management site layout based on improved genetic algorithm[J]. Systems And Soft Computing, 2024, 6: 200113. https://doi.org/10.1016/j.sasc.2024.200113.

[14] Elsheikh A, Motawa I, Diab E. Multi-objective genetic algorithm optimization model for energy efficiency of residential building envelope under different climatic conditions in Egypt[J]. The International Journal of Construction Management, 2023, 23(7/9): 1-10. https://doi.org/10.1080/15623599.2021.1966709.

[15] Yu J, Feng Q, Zhang L. Intelligent City Construction Resource Optimization and Scheduling Algorithm Based on T-S Fuzzy Neural Network and Deep Data Mining[J]. Proceedings of the 2024 4th International Joint Conference on Robotics and Artificial Intelligence, 2024: 5-9.https://doi.org/10.1145/3696474.3696476.

[16] Liu Y. Intelligent Building Optimization Design Based on Artificial Neural Network with Tasmanian Devil Optimization[J]. 2024 International Conference on Intelligent Algorithms for Computational Intelligence Systems (IACIS), 2024: 1-4. https://doi.org/10.1109/iacis61494.2024.10721806.

[17] Wu S, Zhou Z, Wu S. Construction of an Intelligent Decision System for Building Construction Management Risk Based on PSO Algorithm[J]. 2023 International Conference on Integrated Intelligence and Communication Systems (ICIICS), 2023: 1-6. https://doi.org/10.1109/iciics59993.2023.10421285.

[18] Wu C, Lin Y. Intelligent Building Space Layout and Optimization Design Method Based on Biological Population Simulation[J]. Journal of Sensors, 2022, 2022: 6246576. https://doi.org/10.1155/2022/6246576.